Radiation Physics and Chemistry 142 (2018) 60–64

Contents lists available at ScienceDirect

Radiation Physics and Chemistry

journal homepage: www.elsevier.com/locate/radphyschem

Radiation-induced preparation of core/shell gold/albumin nanoparticles

Constanza Y. Flores, Estefania Achilli, Mariano Grasselli*

Laboratorio de Materiales Biotecnológicos (LaMaBio), GBEyB, Grupo Vinculado IMBICE-CONICET; Departamento de Ciencia y Tecnología, Universidad Nacional de Quilmes, Roque Saenz Peña 352, B1876BXD Bernal, Buenos Aires, Argentina

ABSTRACT

Nanoparticles (NPs) are one of the most promising nanomaterials to be used in the biomedical field. Gold NPs (Au-NPs) have been covered with monolayers of many different molecules and macromolecules to prepare different kinds of biosensors. However, these coatings based on physisorption methods are not stable enough to prepare functional nanomaterials to be used in complex mixtures or in vivo applications.

The aim of this work was to prepare a protein coating of Au-NPs based on a protein multilayer covering, stabilized by a novel radiation-induced crosslinking process. Albumins from human and bovine source were added to Au-NPs suspension and followed by ethanol addition to induce protein aggregation. Samples were irradiated with a gamma source at 10 kGy to induce a protein crosslinking according to recent findings. Samples containing 30%v/v ethanol showed a plasmon peak at about 532 nm, demonstrating the presence of non-aggregated Au-NPs. Using higher ethanol concentrations, the absorbance of plasmon peak showed NP aggregation. By Dynamic Light Scattering measurements, a new particle population with an average diameter of about 60 nm was found. Moreover, TEM images showed that the NPs had spherical shape and the presence of a low-density halo around the metal core confirmed the presence of the protein shell. An irradiation dose of one kGy was enough to show changes in the plasmon peak characteristics. The increase in the chemical stability of protein shell was demonstrated by the reduction in the NP dissolution kinetics in presence of cyanate.

1. Introduction

Novel optical effects, very high surface to volume ratios, and different chemical reactivity of surface atoms are some of the features that can be found in nanomaterials. These could be prepared from the same 'classical' materials which at least one of the three special dimensions is ordered in the nanoscale range. The application of these properties to medicine is based on the generation of smart nanostructures, also called nanomedicine, which can combine therapeutic and diagnostic functions within the same entity, which is also called theranostic agent.

One of the most promising nanomaterials in this field is the nanoparticle (NP) prepared from different materials, such as metals, oxides, semiconductors, polymers and others (Kumar, 2007; Sperling and Parak, 2010).

Ionizing radiation has a huge potentiality for generating nanostructures in a straightforward manner, such as the preparation polypeptide-templated Au-NPs (Walker et al., 2013). In this field, our laboratory has reported the preparation of NPs by radiation-induced cross-linking of globular proteins for the first time (Soto Espinoza et al., 2012). This method involves a conjugation of two effects; a dynamic aggregation of native serum albumins (Alb) by a cosolvent addition; and a protein crosslinking induced by irradiation with gamma rays (Achilli et al., 2015). Tailoring size of the NPs can be reached by changing the cosolvent amount in the sample preparation. It is valuable that, according to spectroscopic studies, these Alb-NPs retain a large percentage of the native structure of proteins that comprise them (Soto Espinoza et al., 2012).

However, as a consequence of the organic composition, Alb-NPs have not shown any of the most outstanding physicochemical properties of nanomaterials such as plasmon resonance or magnetic properties. Therefore, in this report it is described the preparation of a core/shell Au/Alb-NPs, in order to improve the Alb-NPs features. It is expected that the novel NPs should have advantages of both materials, such as biophysical and biorecognition properties of proteins and the physicochemical properties of gold nanoparticles.

Surface modification of gold nanoparticles (Au-NPs) with different biomolecules has been used for several decades in rapid diagnostics tests. These are one of the most studied nanomaterials for (bio) chemical sensing and diagnosis. In last years, Au-NPs have proved to be useful in therapy, imaging and delivery applications (Boisselier and Astruc, 2009; Ghosh and Pal, 2007; Janib et al., 2010). They are not

* Corresponding author.
E-mail address: mariano.grasselli@unq.edu.ar (M. Grasselli).

http://dx.doi.org/10.1016/j.radphyschem.2017.02.030
Received 10 October 2016; Received in revised form 17 January 2017; Accepted 12 February 2017
Available online 14 February 2017
0969-806X/

only able to undergo oxidation but very efficiently, transform electromagnetic energy (visible/NIR) into thermal energy. Moreover, it is very stable and the human body is capable of tolerating an amount of grams of this material without side-effects (Nie and Chen, 2012). Those characteristics will allow generating nanomaterials as platform for therapy and diagnoses, or combination of both, thus theranostic NPs. And further, the possibility of using the isotope ^{198}Au as raw material of Au-NP preparation may generate a nanomaterial with radioactive properties, which can emit beta and gamma rays to the milieu (Janib et al., 2010; Park et al., 2012; Xie et al., 2010).

Targeting of NP to specific cell receptors and tumour tissues gives rise to specific interactions in order to localize the theranostic effect on some specific cells and focus the therapy. However, there are still non-specific interactions through other proteins which strongly reduce the NP enrichment in the target. Also, it has been recently recognized that the surface of the NPs and their interaction with proteins has a pivotal role in the target in the body given by the interactions between them and the local environment (Saptarshi et al., 2013). Therefore, the coating process became a strategic issue to develop functional nanomaterials.

Au-NP surface has been covered using organic molecules, especially those containing sulphur atoms are very well described in literature (Giljohann et al., 2010). Coating with monolayers of biomacromolecules, such as antibodies and/or DNA, are nowadays commercially used to prepare lateral flow strips for qualitative detection of target analysts (Volkov et al., 2009) and other biosensors (Saha et al., 2012). However, these coatings based on physisorption methods are not stable enough to prepare functional nanomaterials for complex mixtures or *in vivo* applications (Saha et al., 2012).

The aim of this work was to prepare and characterize a novel protein coating of Au-NPs based on a protein multilayer covering. Human serum albumin (HSA) and bovine serum albumin (BSA) have been used for the preparation of Au-NPs shell which is stabilized by a novel radiation-induced crosslinking method.

2. Materials and methods

Gold (III) auric chloride hydrate (HAuCl4. x H2O) and bovine serum albumin, Fraction V (BSA) were obtained from Sigma Aldrich. Human serum albumin (HSA) was kindly donated by Laboratorio de Hemoterapia (UNC). All other reagents used were of analytical grade and performed as received.

Synthesis of Au/AlbNPs was carried out in several steps. First, Au-NPs were prepared according to literature (Frens, 1973). Briefly, Au-NPs were prepared from a chloroauric solution (1 mM) using sodium citrate as reducing agent, according to Frens method. Second, Au-NPs were dispersed in final concentration of 30 mg/mL albumins (BSA and HSA). Then, different amounts of ethanol were added drop-wise onto the protein solution, keeping the temperature at 0 °C under constant stirring. The water/ethanol suspensions containing Alb and Au-NPs were irradiated with gamma-rays (0.5, 1, 2.5, 5 and 10 kGy) of ^{60}Co source (PISI CNEA-Ezeiza). Samples were previously degassed by nitrogen bubbling for few minutes before closing and keeping samples between 0 and 10 °C.

Particle size was determined by two techniques; Dynamic Light Scattering (DLS) and Transmission Electronic Microscopy (TEM). For DLS, the samples were measured at 25 °C using a 90Plus/Bi-MAS particle size analyzer, with a light source of 632.8 nm and a 10-mW laser. Sample for DLS was purified by Size Exclusion Chromatography (SEC) using a Sephadex G-25 (PD-10, GE Healthcare) according to supplier's instructions. Briefly, a PD-10 column is equilibrated with 25 mL of milliQ water by run into the column by gravity. After 2.5 mL of NP sample is added to the column and the eluent is discarded. Then, 3.5 mL of milliQ water was run into the column to elute the NPs from the column. The procedure is completed in less than 15 min. TEM pictures were captured in Centro de Microscopias Avanzadas (CMA) – FCEyN – University of Buenos Aires. Samples were purified by centrifugation at 10,000 rpm for 15 min and redissolved in H_2O desionized before measuring. All measurements were carried out on days 1 and 30 after sample preparation.

UV–visible and FTIR spectroscopies were performed to study the NPs. FTIR spectroscopy was run using a multireflexion ATR module. The spectra were recorded with 64 scans and a 1 cm^{-1} resolution. Data was analyzed by IR Solution Software. UV–vis spectroscopy was recorded with Shimadzu UV160U spectrophotometer.

Crosslinking stability was determined by the NPs dissolution in a presence of cyanide solution. Briefly, 670 µL of NP sample was incubated with 330 µL of KCN 0.2 mM solution at 40 °C at different times. At several times, samples were measured by UV–vis spectrophotometer on microcells of 70 µL to determine the loss of plasmon peak NPs.

3. Results and discussion

Naked gold nanoparticles (Au-NPs) are very sensitive to the environment and they easily agglomerate by the presence of different solutes (Chegel et al., 2012). These changes can be simply followed by the characteristics of the plasmon absorbance in the visible region. Therefore, this can be used as a very sensitive technique to follow the changes in the NP surface.

Albumin and Au-NPs spontaneously interact with a constant affinity in the micromolar range (Brewer et al., 2005). However, albumin, as most of the proteins, partially loses its native conformation when interacting with the highly structured Au-NPs surface (Tsai et al., 2011). Therefore, the protein recognition sites, available on their surface, are partially lost as a consequence of this interaction, affecting the overall bio-reactivity of NPs (Saptarshi et al., 2013). In addition, major drawbacks are found when NPs are used in complex mixtures or *in-vivo* applications. In these cases, there are numerous adsorptions of different proteins where more abundant ones may initially occupy the surface and are subsequently replaced by other proteins having higher binding affinity for the surface. During these release processes of proteins from the NP surface, it is highly possible to acquire an abnormal folding induced by the NP interaction. Such protein conformational changes may either alter the function of the native protein and/or even lead to exposure to non-native epitopes which may result in immunological recognition (Saptarshi et al., 2013).

In order to improve the surface of nanostructured materials based on Au-NPs, in this work it is proposed the preparation of Au-NPs covered with a shell of multilayer Alb by protein aggregation and radiation-induced crosslinking, which is depicted in Fig. 1. It is

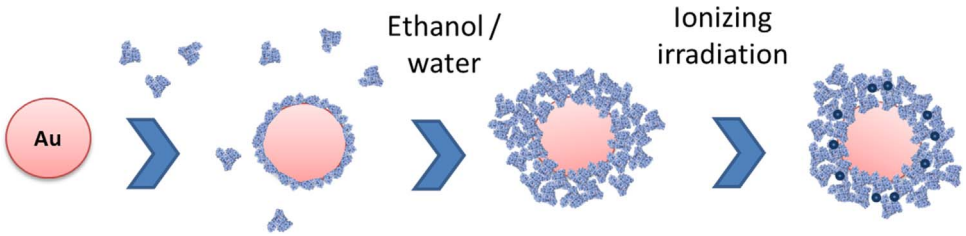

Fig. 1. Scheme of the proposed hybrid NP preparation to yield a core/shell Au/Alb-NPs.

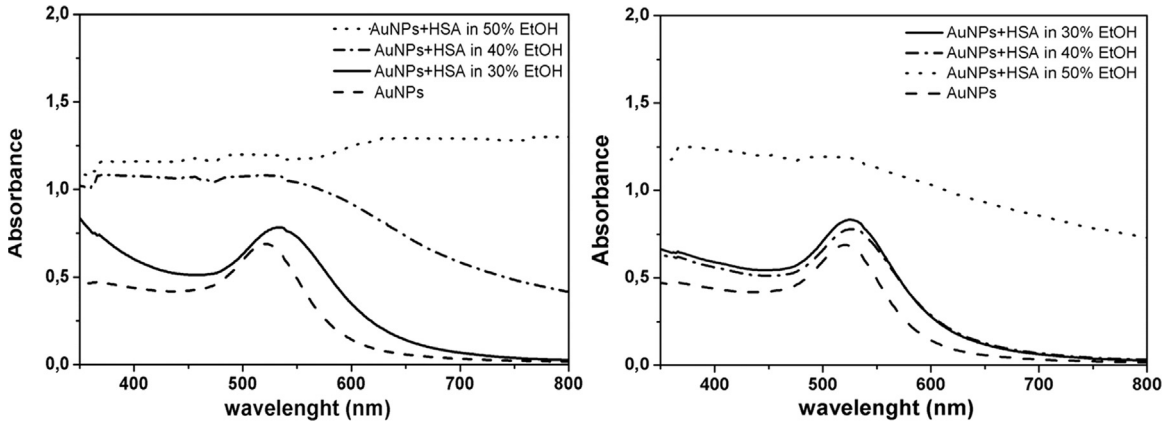

Fig. 2. Visible spectra of (a) the suspension of Au-NPs and HSA 30 mg/mL with the addition of 30%, 40% and 50%v/v ethanol, previous to be irradiated with 10 kGy; and (b) the same samples after irradiation. The plasmon peak corresponding to the naked (citrate capped) Au-NPs was added in both plots for comparison. NP concentration: $2.6.10^{14}$ NPs/l (citrate capped Au-NPs) and $2.2.10^{14}$ NPs/l (all other samples). Optical cell path length:1 cm.

expected a multilayer coating nanomaterial to potentially reduce the protein denaturation of the exposed proteins onto the external layers of the NPs.

This proposed preparation method involved the combination of Au-NP and protein aggregation by cosolvent addition. First, citrate-capped Au-NPs were prepared by chemical reduction of Au salt in aqueous medium by a standard method (Frens, 1973). Albumin solution was added to Au-NPs suspension, where a monolayer of protein coating would be spontaneously formed (Brewer et al., 2005). It was also expected some protein denaturation onto the Au-NP surface and a high excess of protein in solution, according to previous findings (Tsai et al., 2011). In a further step, cold ethanol was added to induce a dynamic protein aggregation, as previously reported for protein NPs preparation (Achilli et al., 2015). To study the described method, the absorbance of Au-NP plasmon was followed in the range of 300–800 nm (see Fig. 2a). The progressive addition of ethanol to the Au-NPs and Alb mixture did not change the plasmon absorbance maximum up to 40% of ethanol. Further ethanol concentration induced the loss of the plasmon characteristic peak as a consequence of the NP agglomeration.

These water/ethanol suspensions, containing BSA and Au-NPs, were irradiated in a ^{60}Co source at 10 kGy dose (1 kGy dose rate) under oxygen free atmosphere and keeping the irradiation temperature below 10 °C. In Fig. 2b the Au-NP plasmon absorbance after the irradiation process is shown. Samples containing 40%v/v and 50%v/v ethanol showed a progressive loss of the plasmon absorbance behaviour; whereas the sample containing only 30%v/v ethanol kept the plasmon signal shape. However, an important shift of the plasmon maximum to higher wavelength (red shift) of 10 nm approximately was recorded. Also, the intensity of plasmon was increased at 14%. These shifts suggested that modifications on NP surfaces occurred. According to our previous findings, similar amount of ethanol was required to generate protein-NPs by radiation-induced cross-linking method (Soto Espinoza et al., 2012).

Different amounts of BSA added to the Au-NPs suspension were studied for the preparation of Au/AlbNPs. No shifts in the maximum plasmon peak were found for coated NPs prepared with protein concentrations in the range of 5–30 mg/mL. However, a small reduction in the plasmon absorbance intensity was recorded for higher protein concentrations (data not shown) rather than for lower concentrations of proteins. This behaviour has also been reported for other molecules (Ghosh and Pal, 2007; Link and El-Sayed, 1999).

In order to confirm the protein coating around the Au-NPs, TEM images were captured using a protein staining to visualize that as well as the Au core. In Fig. 3a and b the pictures corresponding to naked (citrate coated) Au-NPs and Au/BSANPs are shown. A cloudy background of free albumins can also be found. In Fig. 3c and d the protein shell structure around the Au core can be clearly seen. These halos were not visible in TEM pictures without stain (pictures not shown).

In this work SEC procedure was chosen to remove low molecular weight impurities (such as ethanol) with a small sample dilution. Centrifugation is other purification method that can be applied to purify NPs; however a partial NP aggregation has been found. In Fig. 4 the DLS histogram corresponding to the irradiated sample is shown. Two main populations were found corresponding to particles in the range of 10–30 nm and others in the range of 45–80 nm. The first population was assigned to protein-NPs without the Au core and Au/Alb-NPs. To remove the protein-NPs, samples were purified by centrifugation/resuspension cycles (three times) using a microcentrifuge. DLS measurements of samples prepared with different ethanol concentrations showed a main peak depicted in Table 1. The average particle-diameter size increased exponentially with the percentage of ethanol in the suspension. Also the dispersion of NP size was very broad in samples with 40%v/v ethanol or higher. Only 30%v/v ethanol showed an increment to two/three folds in the particle size respect to the citrate-coated Au-NP mean diameter.

Visible spectra corresponding to the irradiated Au/BSA-NP suspension crude or purified sample showed the same shift of the plasmon absorbance peak (data not shown).

FT-IR spectroscopy analysis was performed onto BSA, AuNPs and Au/BSA NPs. The core/shell NP spectrum shows two main peaks corresponding to the amide regions I and II, respectively. These peaks were confirmed by running BSA sample, corroborating the presence of albumin layers onto the AuNP surface.

In the following experiment the minimum irradiation dose was determined using a sample containing 30%v/v ethanol. Samples were prepared using the same concentration of Au-NPs and Alb corresponding to the previous experiment. In Fig. 5 it is plotted the changes in the plasmon absorbance peak as a function of the irradiation dose, in the range of 0–10 kGy. All samples were irradiated at a dose rate of 1 kGy/h. Two plasmon absorbance parameters were analyzed, the maximum of the plasmon peak wavelength and the relative peak intensity (respective to the same non-irradiated sample). The maximum peak wavelength showed a transition from 528 ± 2 nm to 534 ± 2 nm. A sharp change of this parameter occurred in the range of 0.5–1 kGy. The other parameter, the relative absorbance of the maximum peak decreased from 0.97 to 0.83 ± 0.07, when the total irradiation dose increased. As plotted in Fig. 5, the change in absorbance took place in the same dose as the other variable. This minimum dose value was lower than the irradiation dose required to prepare BSA-NPs by electron-beam irradiation (Achilli et al., 2015). Therefore, it can be speculated that Au-NP core captured some of the energy and released it for the crosslinking process.

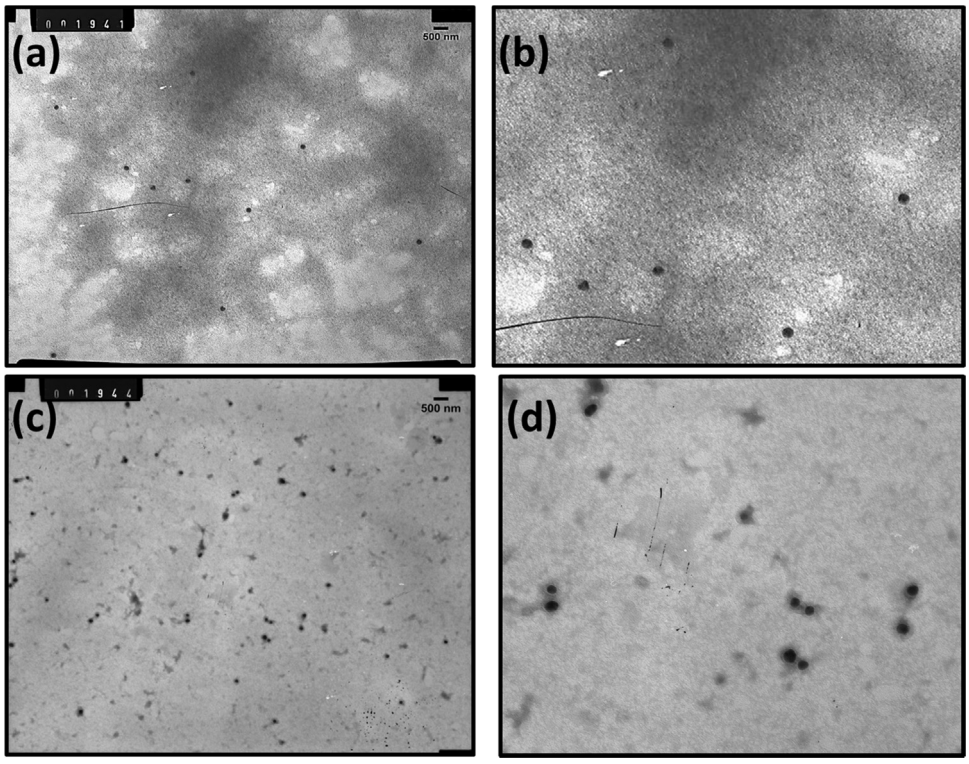

Fig. 3. TEM pictures of (a) and (b) a suspension of Au-NPs and HSA 30 mg/mL previous to be irradiated with 10 kGy; and (c) and (d) the same samples after irradiation. Figures (a) and (c) have a 100,000×magnification and (b) and (d) are zoom same images.

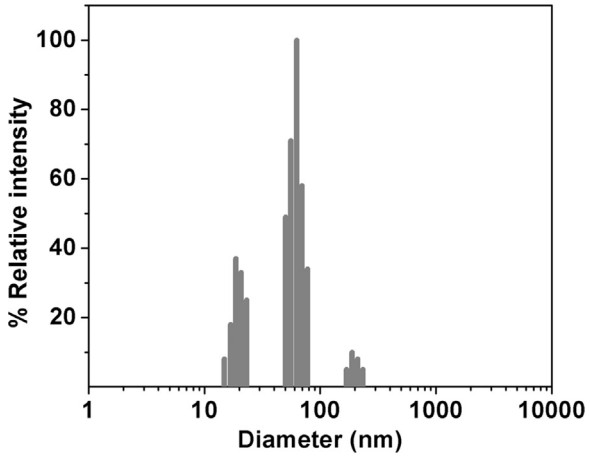

Fig. 4. DLS histogram corresponding to an Au/Alb-NP purified by Size Exclusion Chromatography. HSA: 30 mg/mL; Ethanol: 30%v/v; Irradiation dose: 10 kGy.

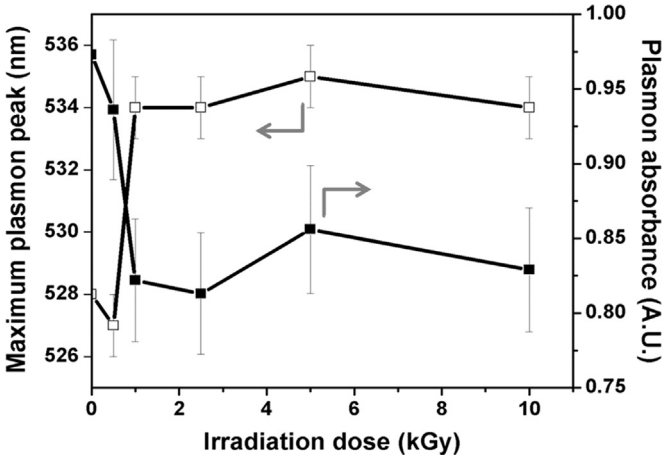

Fig. 5. Plasmon peak characteristics for different irradiation doses. Left abscissa axis represents the maximum peak wavelength (open square) and right abscissa axis represents the absorbance of the plasmon peak (close square).

Table 1
Mean diameter of NPs prepared by radiation-induced crosslinking method (Average ± 1 SD) of Au-NPs (citrate-capped) with HSA 30 mg/mL and ethanol in different concentrations.

NP preparation	Diameter (nm)
Au-NPs	33 ± 10
Au-NPs+HSA in 30% EtOH	78 ± 5
Au-NPs+HSA in 40% EtOH	5650 ± 4000
Au-NPs+HSA in 50% EtOH	6400 ± 5000

Au-NPs can be easily dissolved using a cyanide solution, transforming the red suspension of Au-NPs in a light-yellow colour of the solution of auric ions (Demers et al., 2000). Taking into account that irradiation with a ^{60}Co source generates crosslinking in the protein shell of Au/BSA-NPs, there is a difference in permeation rate of cyanide ions through them. It should be shown different dissolution behaviour from the Au core. In Fig. 6a it is shown the kinetic of dissolution measured as the disappearance of plasmon absorption peak at 40 °C. To standardize all conditions, it was plotted the relative absorbance of Au/BSA-NPs, prepared at different irradiation dose, respect to the same sample without addition of cyanide. In the period of three hours, citrate-coated Au-NPs (or naked) were completely dissolved; meanwhile all the irradiated samples showed slower dissolution behaviour (Fig. 6a). In Fig. 6b it is plotted the NP dissolution %, determined as the percentage of variation of plasmon peak after 30 min within cyanide solution. Considering this parameter, the sample irradiated with the minimum dose studied (0.5 kGy) showed a high differential dissolution respect to the non-irradiated one; and all the other samples, ranged from 1 and 10 kGy, showed a dissolution rate difference lower than ten percent.

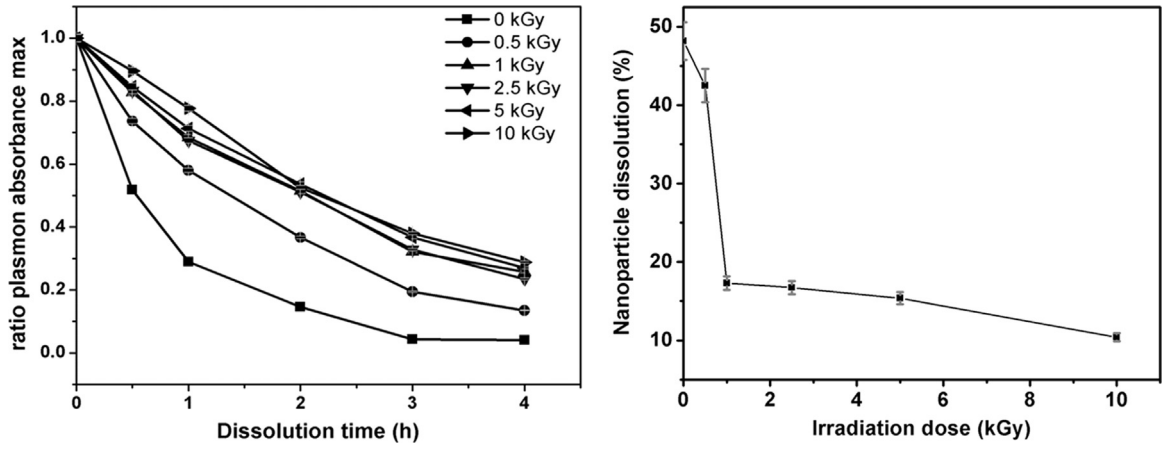

Fig. 6. Nanoparticle dissolution test. (a) Ratio of plasmon peak maximum with the incubation time in a cyanate solution. (b) Percentage of the nanoparticle dissolution at 30 min of incubation time with cyanate solution versus the irradiation dose.

4. Conclusions

Ionizing radiation is a well-known industrial tool for crosslink processing of polymers. Proteins are very sophisticated polymers from biological source. The deleterious effect of ionizing irradiation onto aqueous protein solutions restricted its application onto these proteinaceous materials. In recent years it was found that the use of aqueous/ethanol solvent in samples containing proteins enhanced the crosslinking and drastically reduced their degradation effects.

Proteins are biological polymers with the main property of their reproducible ensemble in predetermined spatial conformation at nanoscale level. This feature allows generating functional materials with highly specific properties, such as molecular recognition, and/or catalysing organic reactions. Therefore, the combination of protein characteristics and the powerful ionizing radiation to generate chemical crosslinking without additional chemicals opens the possibility of preparating novel protein-based nanostructures straightforwardly. In this work we extended the radiation-based method used for preparation of protein NPs to create protein coatings of Au-NPs in a multilayer fashion.

According to the experimental data showed in this report hybrid NPs were prepared based on Au-NPs and proteins. Au-NPs were covered with a multilayer of Alb and stabilized by a novel method which involved a radiation-induced crosslinking process. Alb solution was previously added to Au-NP suspension and partially aggregated by the addition of certain amount of cosolvent. Samples were irradiated in a ^{60}Co source to stabilize the nanoconstructs by radiation-induced crosslinking. Plasmon absorbance, DLS and TEM images were compatible with the proposed core / shell hybrid material depicted in Fig. 1. Albumin coating did not interfere with the optical properties of Au-NPs and, according to preliminary studies; they showed higher chemical stability.

In further studies, this hybrid Au/Alb-NPs will be functionalized with peptides for improvement of the specific cell bio recognition.

Acknowledgements

MG is member of the National Council of Scientific and Technical Research (CONICET), and CF and EA would like to thank CONICET for their fellowships. The research leading to these results has received partial funding from and the Nuclear Atomic Energy Agency –IAEA (CRP code F22064), Argentinean grants from Ministry of Science, Technology and Productive Innovation (MINCYT) and Universidad Nacional de Quilmes (UNQ), Buenos Aires, Argentina.

References

Achilli, E., Casajus, G., Siri, M., Flores, C., Kadłubowski, S., Alonso, S. d.V., Grasselli, M., 2015. Preparation of protein nanoparticle by dynamic aggregation and ionizing-induced crosslinking. Colloids Surf. A: Physicochem. Eng. Asp. 486, 161–171.
Boisselier, E., Astruc, D., 2009. Gold nanoparticles in nanomedicine: preparations, imaging, diagnostics, therapies and toxicity. Chem. Soc. Rev. 38 (6), 1759–1782.
Brewer, S.H., Glomm, W.R., Johnson, M.C., Knag, M.K., Franzen, S., 2005. Probing BSA binding to citrate-coated gold nanoparticles and surfaces. Langmuir 21 (20), 9303–9307.
Chegel, V., Rachkov, O., Lopatynskyi, A., Ishihara, S., Yanchuk, I., Nemoto, Y., Hill, J.P., Ariga, K., 2012. Gold nanoparticles aggregation: drastic effect of cooperative functionalities in a single molecular conjugate. J. Phys. Chem. C 116 (4), 2683–2690.
Demers, L.M., Mirkin, C.A., Mucic, R.C., Reynolds, R.A., Letsinger, R.L., Elghanian, R., Viswanadham, G., 2000. A fluorescence-based method for determining the surface coverage and hybridization efficiency of thiol-capped oligonucleotides bound to gold thin films and nanoparticles. Anal. Chem. 72 (22), 5535–5541.
Frens, G., 1973. Controlled nucleation for the regulation of the particle size in monodisperse gold suspensions. Nature 241 (105), 20–22.
Ghosh, S.K., Pal, T., 2007. Interparticle coupling effect on the surface plasmon resonance of gold nanoparticles: from theory to applications. Chem. Rev. 107 (11), 4797–4862.
Giljohann, D.A., Seferos, D.S., Daniel, W.L., Massich, M.D., Patel, P.C., Mirkin, C.A., 2010. Gold Nanoparticles for Biology and Medicine. Angew. Chem. Int. Ed. 49 (19), 3280–3294.
Janib, S.M., Moses, A.S., MacKay, J.A., 2010. Imaging and drug delivery using theranostic nanoparticles. Adv. Drug Deliv. Rev. 62 (11), 1052–1063.
Kumar, C.S., 2007. Nanomaterials for Cancer Diagnosis. Wiley-VCH, Weinheim.
Link, S., El-Sayed, M.A., 1999. Size and Temperature Dependence of the Plasmon Absorption of Colloidal Gold Nanoparticles. J. Phys. Chem. B 103 (21), 4212–4217.
Nie, X., Chen, C., 2012. Au nanostructures: an emerging prospect in cancer theranostics. Sci. China Life Sci. 55 (10), 872–883.
Park, S.H., Lee, J.H., Lee, G.-B., Byun, H.-J., Kim, B.-R., Park, C.-Y., Kim, H.-B., Rho, S.B., 2012. PDCD6 additively cooperates with anti-cancer drugs through activation of NF-κB pathways. Cell. Signal. 24 (3), 726–733.
Saha, K., Agasti, S.S., Kim, C., Li, X., Rotello, V.M., 2012. Gold nanoparticles in chemical and biological sensing. Chem. Rev. 112 (5), 2739–2779.
Saptarshi, S.R., Duschl, A., Lopata, A.L., 2013. Interaction of nanoparticles with proteins: relation to bio-reactivity of the nanoparticle. J. Nanobiotechnol. 11 (1), 1.
Soto Espinoza, S.L., Sánchez, M.L., Risso, V., Smolko, E.E., Grasselli, M., 2012. Radiation synthesis of seroalbumin nanoparticles. Radiat. Phys. Chem. 81 (9), 1417–1421.
Sperling, R.A., Parak, W.J., 2010. Surface modification, functionalization and bioconjugation of colloidal inorganic nanoparticles. Philos. Trans. R. Soc. A: Math. Phys. Eng. Sci. 368 (1915), 1333–1383.
Tsai, D.-H., DelRio, F.W., Keene, A.M., Tyner, K.M., MacCuspie, R.I., Cho, T.J., Zachariah, M.R., Hackley, V.A., 2011. Adsorption and conformation of serum albumin protein on gold nanoparticles investigated using dimensional measurements and in situ spectroscopic methods. Langmuir 27 (6), 2464–2477.
Volkov, A., M. Mauk, P. Corstjens and R. S. Niedbala (2009). Rapid Prototyping of Lateral Flow Assays. Biosensors and Biodetection. A. Rasooly and K. Herold, Humana Press. **504:** pp. 217–235.
Walker, C.R., Pushpavanam, K., Nair, D.G., Potta, T., Sutiyoso, C., Kodibagkar, V.D., Sapareto, S., Chang, J., Rege, K., 2013. Generation of polypeptide-templated gold nanoparticles using ionizing radiation. Langmuir 29 (32), 10166–10173.
Xie, J., Lee, S., Chen, X., 2010. Nanoparticle-based theranostic agents. Adv. Drug Deliv. Rev. 62 (11), 1064–1079.